

BRIDGING THE GAP: A SOFTWARE TOOL FOR EFFICIENT GROUND MOTION RECORD SELECTION IN EARTHQUAKE ENGINEERING

Davit Shahnazaryan ⁽¹⁾, Volkan Ozsarac ⁽²⁾, Gerard J. O'Reilly ⁽³⁾

⁽¹⁾ Postdoctoral Researcher, Centre for Training and Research on Reduction of Seismic Risk (ROSE Centre), Scuola Universitaria Superiore IUSS Pavia, Pavia, Italy. E-Mail: davit.shahnazaryan@iusspavia.it

⁽²⁾ Postdoctoral Researcher, Centre for Training and Research on Reduction of Seismic Risk (ROSE Centre), Scuola Universitaria Superiore IUSS Pavia, Pavia, Italy. E-Mail: volkan.ozsarac@iusspavia.it

⁽³⁾ Associate Professor, Centre for Training and Research on Reduction of Seismic Risk (ROSE Centre), Scuola Universitaria Superiore IUSS Pavia, Pavia, Italy. E-Mail: gerard.oreilly@iusspavia.it

Abstract

With the significant advancements in computational power in recent decades, non-linear response history analysis has become more prevalent in seismic design and assessment. A critical step in these applications is the selection and scaling of appropriate ground motion records. However, state-of-the-art record selection procedures are rarely employed by engineers due to the lack of user-friendly and computationally efficient software tools, despite the advances in know-how in the research community. To address these challenges, a user interface (UI)-based software for ground motion record selection is introduced. In addition to the traditional building code-compliant approaches, the software integrates the generalised conditional intensity measure (GCIM) framework to select hazard-consistent records from harmonised databases, such as the PEER NGA-West2, and to provide corresponding scale factors. This approach allows for a combined consideration of any number of ground motion intensity measure types through cross-correlation matrices. Furthermore, the multiple causal earthquakes and ground motion models (GMMs) can be incorporated, as done in the probabilistic seismic hazard analysis (PSHA). The application of the tool is demonstrated using a generalised GMM to facilitate efficient record selection. The UI is designed for ease of use allowing flexibility for users to switch between the different methods of selection and retention of input and output data. The tool supports the selection of both horizontal and vertical ground motion components. A case study is presented demonstrating the performance of the tool for conditional and unconditional selection.

Keywords: ground-motion record selection, conditional selection, unconditional selection, code-based selection, graphical user interface.

1. Introduction

The selection of ground motion records in seismic design and assessment applications needs to be approached with great care, as it can have direct impact on the accuracy and the reliability of seismic performance evaluations. This process begins with defining a ‘target’, which, among others, could be the design response spectrum specified in building codes worldwide, a uniform hazard spectrum (UHS) derived from a probabilistic seismic hazard analysis (PSHA) [1], or a weighted average of response spectra from earthquake scenarios conditioned on a specific spectral acceleration ordinate ([2], [3]). Selection algorithms are then employed to identify a suite of records whose response spectra closely match this ‘target’ based on the specified criteria. Specifically, when the target is a Conditional Spectrum (CS), the selected suite achieves hazard consistency by ensuring that the distributions of response spectra from the selected ground motions are consistent with the hazard curves at all relevant periods. Over the years, numerous ground motion selection methods have been proposed in the literature to account for both the mean and variability of response spectra corresponding to such ‘targets’ ([4], [5]).

In general, all ground motion record selection methods rely on the elastic spectral accelerations of ground motions. However, it is well understood that the severity of ground motion also depends on

factors such as intensity, velocity, duration, and frequency content. To address the limitations of these traditional methods, Bradley ([6], [7]) introduced the generalised conditional intensity measure (GCIM) approach, which allows the distribution of a ground motion intensity measure (IM) to be derived based on the values of other IMs. One notable characteristic or ‘limitation’ (at the time of introduction) of GCIM was the reliance on ground motion models (GMMs) to estimate the distribution of expected ground motion intensities and their associated uncertainties given a set of causal parameters (e.g., magnitude, source-to-site distance). Initially, the GCIM approach could only accommodate a limited number of IMs, such as spectral acceleration, peak ground acceleration, Arias intensity, or significant duration. However, advancements in GMM development in recent years have transformed this perceived limitation into a significant strength. For example, newer GMMs have been developed for cumulative intensity-based IMs (e.g., significant duration) and amplitude-based IMs (e.g., spectral acceleration), with these models predicting the IMs independently ([8]–[11], among others). Recent research has focused on developing GMMs for next-generation IMs, such as filtered incremental velocity (*FIV3*) [12] and average spectral acceleration (Sa_{avg}) [13], which have demonstrated promising efficiency and sufficiency ([14]–[16]). Furthermore, Aristeidou et al. [17] proposed a GMM capable of predicting a wide range of IMs using a single model, further enhancing the applicability of the GCIM framework.

Ground motion selection procedures rely not only on the availability of relevant GMMs but also on the correlations between the IMs (or the spectral ordinates of the same IM). To derive the conditional distribution of one IM with respect to others, these correlations are essential. Addressing this need, Aristeidou et al. [18] developed correlation models that account for both traditional IMs (such as spectral acceleration, peak ground acceleration, peak ground velocity, and significant duration) and next-generation IMs (e.g., *FIV3*, Sa_{avg}).

With substantial advancements in computational power over recent decades, along with progress in GMMs, correlation models, and ground motion record selection procedures, non-linear response history analysis has become increasingly prominent in seismic design and assessment. In fact, it is the preferred method of design verification and assessment for practising engineers worldwide due to its perceived accuracy and insights given into the seismic behaviour of structures. Despite these developments, engineers rarely utilise advanced record selection methods due to the lack of accessible and efficient software tools. To address this gap, this paper presents a user interface (UI)-based software tool for ground motion record selection. Beyond conventional approaches that adhere to building code requirements, the software also allows for vertical component selection and integrates the GCIM framework to select records from harmonised databases such as PEER NGA-West2 [19], while also providing corresponding scale factors. This approach allows for the simultaneous consideration of multiple ground motion IMs using cross-correlation matrices. Furthermore, the tool accommodates multiple causal earthquakes and GMMs, as is standard practice in PSHA. The software’s functionality is demonstrated through the application of a generalised GMM [17], facilitating efficient record selection. Finally, a case study compares the performance of unconditional and conditional selection methods.

2. Probabilistic seismic hazard analysis

Before initiating the ground motion selection procedure, it is essential to identify target response spectra for the selection process. A commonly accepted approach for defining these target spectra involves performing PSHA. To conduct PSHA, rupture parameters (*rup*) and GMMs (*gmm*) are required. These inputs form the basis of a logic tree, which is used to capture and quantify epistemic uncertainty associated with the PSHA inputs. Figure 1 illustrates an example of this process, demonstrating how different GMMs are utilised to model two distinct rupture scenarios in constructing a target spectrum. Throughout this document, it is assumed that the rupture parameters and their corresponding GMMs for each IM of interest are predefined and readily available as provided by PSHA disaggregation. Figure 2 illustrates a sample disaggregation output following PSHA for a return period of 4975 years. The disaggregation of hazard from all sources is typically obtained by accumulating magnitude and distance bin contribution to the global hazard. In the example, the highest contribution is controlled by an event

of magnitude 7.38 and a distance of 1km. This assumption facilitates the consideration of various rupture scenarios and associated GMMs in the calculations, aligning with standard practices in PSHA. For each rupture scenario rup_r , the associated probability p_r is known, such that:

$$\sum_{r=1}^{n_{rup}} p_r = 1 \quad (1)$$

And for each gmm_g used to model this rup_r , its associated weights, $w_{r,g}$, are given:

$$\sum_{g=1}^{n_{gmm}^r} w_{r,g} = 1 \quad (2)$$

where n_{gmm}^r is the number of GMMs used to model rup_r . All rup and associated gmm are assumed to be considered in the target identification, which is generally referred to in the literature as the *exact* approach, described by Lin et al. [3]. The *approximate* approach, is a special case where one single rup is modelled using a single gmm , therefore implying that $p_1=w_{1,1}=1.0$.

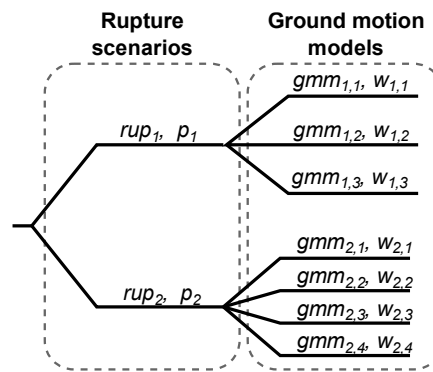


Figure 1. Different rupture scenarios and GMMs that may be considered.

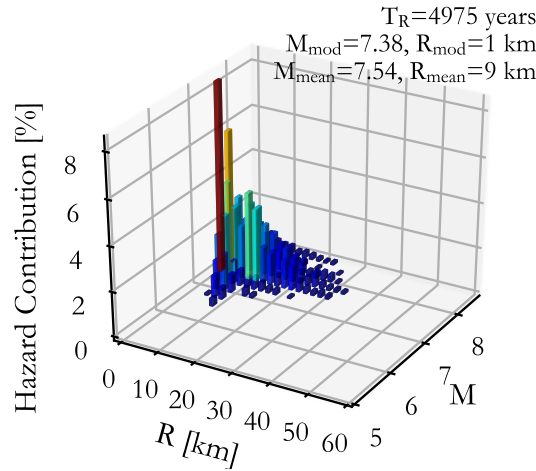


Figure 2. Sample illustration of disaggregation results from PSHA.

3. Target identification

3.1. Unconditional spectrum

Following the setup of the logic tree, first an approximate case with only a single rupture scenario and GMM is employed. In this case, the unconditional mean and variance are computed using Eq. (3) and Eq. (4).

$$\mu_{\ln IM_i} = \mu_{\ln IM_i^g | rup_r} \quad (3)$$

$$\sigma_{\ln IM_i}^2 = \sigma_{\ln IM_i^g | rup_r}^2 \quad (4)$$

where $\mu_{\ln IM_i^g | rup_r}$ and $\sigma_{\ln IM_i^g | rup_r}^2$ are the mean and variance of the natural logarithm of a known IM, IM_i , for a single rupture rup_r , and GMM gmm_g . The approximate case may be generalised to consider for many different rupture scenarios and GMMs, as a result the unconditional mean and variance are obtained using Eq. (5) and Eq. (6).

$$\mu_{\ln IM_i} = \sum_{r=1}^{n_{rup}} \sum_{g=1}^{n_{gmm}^r} p_r w_{r,g} \mu_{\ln IM_i^g | rup_r} \quad (5)$$

$$\sigma_{\ln IM_i}^2 = \sum_{r=1}^{n_{rup}} \sum_{g=1}^{n_{gmm}^r} p_r w_{r,g} \left(\sigma_{\ln IM_i^g | rup_r}^2 + \left(\mu_{\ln IM_i} - \mu_{\ln IM_i^g | rup_r} \right)^2 \right) \quad (6)$$

Lin et al. [3] termed those as *exact* and *approximate* approaches, and presented four different methods to compute a target response spectrum. The different between each method depends on the hazard input cases considered.

- Method 1 involves a single GMM applied to a single rupture scenario (i.e., $n_{rup} = n_{gmm}^r = 1$).
- Method 2 considers multiple GMMs for the same rupture scenario (i.e., $n_{rup} = 1, n_{gmm}^r > 1$). In this approach, the GMM weights, $w_{1,g}$, are derived from the PSHA logic tree (i.e., $p_r = 1, w_{1,g} = w_{1,g}^l$, where l refers to the logic tree).
- Method 3 considers a single rupture scenario for each GMM (i.e., $n_{rup} = n_{gmm} > 1$). Here, the GMM weights, $w_{r,g}$, are obtained from PSHA disaggregation (i.e., $p_r w_{r,g} = p_r^d w_{r,g}^d$, with d signifying disaggregation).
- Method 4 follows a more generalised framework, adhering to the formulations provided in Eq. (5) and Eq. (6).

These methods underscore the varying levels of complexity and the different considerations for hazard inputs in target response spectrum computation. It is crucial to note that the weights derived from PSHA disaggregation (i.e., $p_r^d, w_{r,g}^d$) differ from the logic tree weights (i.e., $p_r^l, w_{r,g}^l$). Lin et al. [3] discusses how the logic tree weights are analogous to prior weights in decision analysis, while disaggregation weights correspond to posterior weights. Moreover, disaggregation weights are typically expressed as a single product, $p_r^d w_{r,g}^d$, rather than as separate components, which are still compatible to the formulations given in Eq. (5) and Eq. (6) and correspond to the *exact* approach.

3.2. Conditional spectrum

In the case of conditional response spectrum dependent on a certain IM, IM^* , as the target for record selection, unconditional means and variances transform to $\mu_{\ln IM_i^g | \ln IM^*h, rup_r}$ and $\sigma_{\ln IM_i^g | \ln IM^*h, rup_r}^2$, respectively. It is assumed that the value of $\ln IM^*h$ will be obtained from another GMM denoted h . Conditional target mean and variance for a given rupture scenario rup_r and GMM pair will be given by the following expressions:

$$\mu_{\ln IM_i^g | \ln IM^*h, rup_r} = \mu_{\ln IM_i^g | rup_r} + \rho_{\ln IM_i^g, \ln IM^*h | rup_r} \sigma_{\ln IM_i^g | rup_r} \epsilon_{\ln IM^*h | rup_r} \quad (7)$$

$$\sigma_{\ln IM_i^g | \ln IM^*h, rup_r}^2 = \sigma_{\ln IM_i^g | rup_r}^2 \left(1 - \rho_{\ln IM_i^g, \ln IM^*h | rup_r}^2 \right) \quad (8)$$

$$\epsilon_{\ln IM^*h | rup_r} = \frac{\ln IM^*h - \mu_{\ln IM^*h | rup_r}}{\sigma_{\ln IM^*h | rup_r}} \quad (9)$$

Baker [2] describes the term, ρ , as the correlation of the residuals, ϵ , of $\ln IM_i^g$ and $\ln IM^*h$, corresponding to two different GMMs, g and h , respectively, and for given rupture parameters rup_r . This definition presumes the availability of a correlation model specific for these two IMs, the

respective GMMs, and the particular rupture parameters rup_r . However, Baker and Bradley [20] supported the idea of a more practical approach by suggesting the omission of the dependence on specific rupture parameters and GMMs when developing correlation models. This simplification facilitates broader applicability without compromising the utility of the correlation models in practical scenarios. As a result, Eq. (7) and Eq. (8) may be rewritten into Eq. (10) and Eq. (11), respectively.

$$\mu_{\ln IM_i^g | \ln IM^{*h}, rup_r} = \mu_{\ln IM_i^g | rup_r} + \rho_{\ln IM_i, \ln IM^*} \sigma_{\ln IM_i^g | rup_r} \epsilon_{\ln IM^{*h} | rup_r} \quad (10)$$

$$\sigma_{\ln IM_i^g | \ln IM^*, rup_r}^2 = \sigma_{\ln IM_i^g | rup_r}^2 (1 - \rho_{\ln IM_i, \ln IM^*}^2) \quad (11)$$

The combined conditional mean spectrum (CMS) is computed as the weighted sum of each:

$$\mu_{\ln IM_i^g | \ln IM^*, rup_r} = \sum_{h=1}^{n_{gmm}^r} w_h \mu_{\ln IM_i^g | \ln IM^{*h}, rup_r} \quad (12)$$

Here, the GMM h is considered individually, meaning that the weights w_h need to be obtained from the logic tree branch for rup_r . For a single rupture scenario, the conditional mean and variance will be given by Eq. (13) and Eq. (14).

$$\mu_{\ln IM_i | \ln IM^*} = \mu_{\ln IM_i^g | \ln IM^*, rup_r} \quad (13)$$

$$\sigma_{\ln IM_i | \ln IM^*}^2 = \sigma_{\ln IM_i^g | \ln IM^*, rup_r}^2 \quad (14)$$

Extending the conditional approach to include multiple rupture scenarios and GMMs, the resulting mean and variance will be given by Eq. (15) and Eq. (16). This represents the full expansion of the GCIM approach for ground motion record selection as proposed by Bradley [6]. The primary distinction lies in the inclusion of multiple rupture scenarios as opposed to the single rupture scenario originally presented in Bradley [6]. Figure 3 presents an example of a conditional selection, illustrating the means and standard deviations of the target, calculated using Eq. (15) and Eq. (16), respectively. This example involves an application with two rupture scenarios and two Ground Motion Models (GMMs). The individual grey dashed branches represent the results obtained from Eq. (12) for the means and Eq. (11) for the standard deviations.

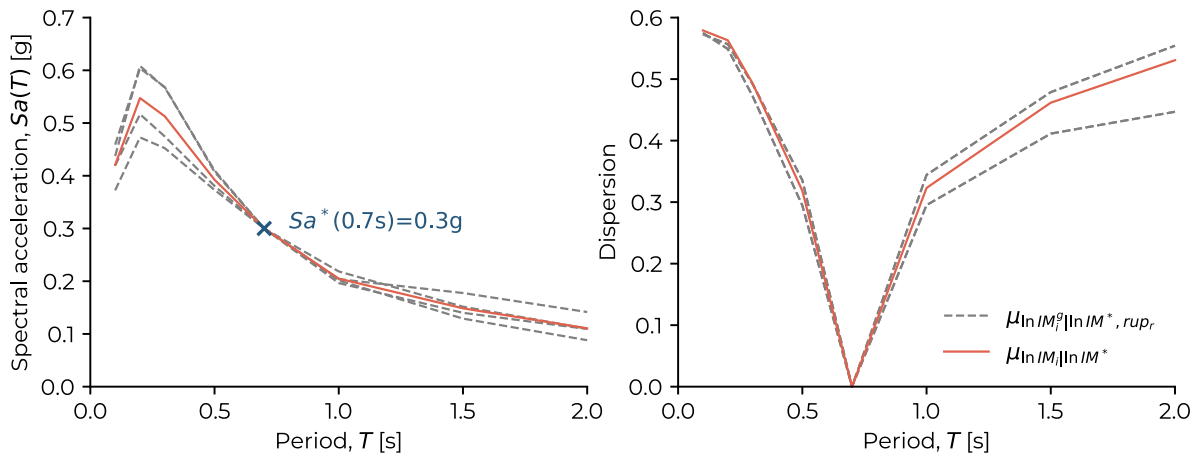


Figure 3. Illustration of (left) means and (right) dispersions computed for a case of two ruptures and two GMMs, where the solid lines represent the mean value and the dashed lines represent the mean plus and minus two standard deviations for a conditional selection

$$\mu_{\ln IM_i | \ln IM^*} = \sum_{r=1}^{n_{rup}} \sum_{g=1}^{n_{gmm}^r} p_r w_{r,g} \mu_{\ln IM_i^g | \ln IM^*, rup_r} \quad (15)$$

$$\sigma_{\ln IM_i | \ln IM^*}^2 = \sum_{r=1}^{n_{rup}} \sum_{g=1}^{n_{gmm}^r} p_r w_{r,g} \left(\sigma_{\ln IM_i^g | \ln IM^*, rup_r}^2 + \left(\mu_{\ln IM_i | \ln IM^*} - \mu_{\ln IM_i^g | \ln IM^*, rup_r} \right)^2 \right) \quad (16)$$

3.3. Simulating targets for ground motion record selection

Once the target means and variances are identified, ground motion records may be selected. Ground motions are selected collectively meaning that both the mean and variance of the group must be matched and not in a piecewise fashion. To resolve this, Jayaram and Baker [21] proposed that suitable ground motion records $\ln IM_i$ are simulated and actual ground motions with values close to these are looked for. To achieve it, the vector of means, $\mu_{\ln IM}$, and the covariance, $\Sigma_{\ln IM}$, of the vector of $\ln \mathbf{IM} = \{ \dots, \ln IM_i, \dots \}$ is used. Those can be written as:

$$\mu_{\ln \mathbf{IM}} = \begin{bmatrix} \vdots \\ \mu_{\ln IM_i | \ln IM^*} \\ \vdots \end{bmatrix} \quad (17)$$

The standard deviation is written as:

$$\sigma_{\ln \mathbf{IM}} = \begin{bmatrix} \vdots \\ \sigma_{\ln IM_i | \ln IM^*} \\ \vdots \end{bmatrix} \quad (18)$$

The correlation between each of the $\ln \mathbf{IM}$ values conditioned on $\ln IM^*$ needs to be computed to fully characterise the multivariate normal distribution parameters. Bradley [7] describes this as:

$$\rho = \begin{bmatrix} \ddots & \dots & \\ \vdots & \rho_{\ln IM_i, \ln IM_j | \ln IM^*} & \vdots \\ & \dots & \ddots \end{bmatrix} \quad (19)$$

where the individual conditional correlation term is given by:

$$\rho_{\ln IM_i, \ln IM_j | \ln IM^*} = \frac{\rho_{\ln IM_i, \ln IM_j} - \rho_{\ln IM_i, \ln IM^*} \rho_{\ln IM_j | \ln IM^*}}{\sqrt{1 - \rho_{\ln IM_i | \ln IM^*}^2} \sqrt{1 - \rho_{\ln IM_j | \ln IM^*}^2}} \quad (20)$$

This is then used to construct the covariance matrix between each of the $\ln \mathbf{IM}$ terms conditioned on $\ln IM^*$ as:

$$\Sigma = \begin{bmatrix} \ddots & \dots & \\ \vdots & \Sigma_{\ln IM_i, \ln IM_j | \ln IM^*} & \vdots \\ & \dots & \ddots \end{bmatrix} \quad (21)$$

where the individual conditional covariance term is given by:

$$\Sigma_{\ln IM_i, \ln IM_j | \ln IM^*} = \rho_{\ln IM_i, \ln IM_j | \ln IM^*} \sigma_{\ln IM_i | \ln IM^*} \sigma_{\ln IM_j | \ln IM^*} \quad (22)$$

4. Ground motion record selection tool

This section presents an online toolbox developed to implement the outlined framework. At this stage, the tool, available at <https://apps.djura.it/hazard/record-selector>, includes several methods, ranging from basic building code requirements to more complex hazard scenarios. However, the building code requirements will not be the focus of this section. The tool enables the selection of records using a set of target spectra for various ground motion IMs, based on specific rupture parameters, a process commonly referred to as scenario-based analysis. Both generalised unconditional and conditional selection options are available. Within the tool, users are required to choose key attributes and functionalities:

1. **IM – GMM Pairs:** IMs must be specified alongside the GMMs required to predict their expected distribution. Figure 4(left) illustrates the interface for this process. For example, when

spectral acceleration, $Sa(T)$, is selected, a menu of available GMMs is displayed. The graphic below dynamically updates to reflect the chosen GMMs and shows their associated weights, which users can adjust as needed. The following IMs are currently supported: $Sa(T)$, average spectral acceleration, $Sa_{avg}(T)$, peak ground acceleration, PGA , peak ground velocity, PGV , significant durations, D_{S575} and D_{S595} , and filtered incremental velocity, $FIV3$.

2. **Rupture Scenarios:** scenario parameters are defined based on the previously selected IMs and GMMs. The site context, which refers to the characteristics of the site of interest rather than the earthquake rupture itself, is specified separately. The most common parameter to characterise a site is the average shear wave velocity to 30 meters depth, V_{S30} . Additional fields such as $Z_{2.5}$ and the soil/rock indicator also appear depending on the GMMs employed. Detailed explanations for each parameter are provided within the tool's interface and references are also provided. Next, rupture parameters are specified, typically derived from the disaggregation results of PSHA. Users often define a single dominant rupture scenario for each intensity level, as is customary in the *approximate* selection approach (Lin et al. [3]). A notable feature of the presented record selector is its ability to manage multiple rupture scenarios by assigning relative weights to each scenario based on PSHA results, a method referred to as the *exact* approach by Lin et al. [3]. Figure 4(right) gives the graphical UI for this process.
3. **Conditional IM (only for conditional selection):** the core concept of conditional ground motion record selection is that the chosen ground motions correspond to a specified value of intensity for a particular IM. This specified value, referred to as the conditioning value, or IM^* , is typically obtained from the hazard curve or PSHA. From the previously selected pool of IMs (from Step 1), the user must choose the conditioning IM and specify its conditioning value. The tool then utilises this value to define the target distribution of the ground motions relative to this point.

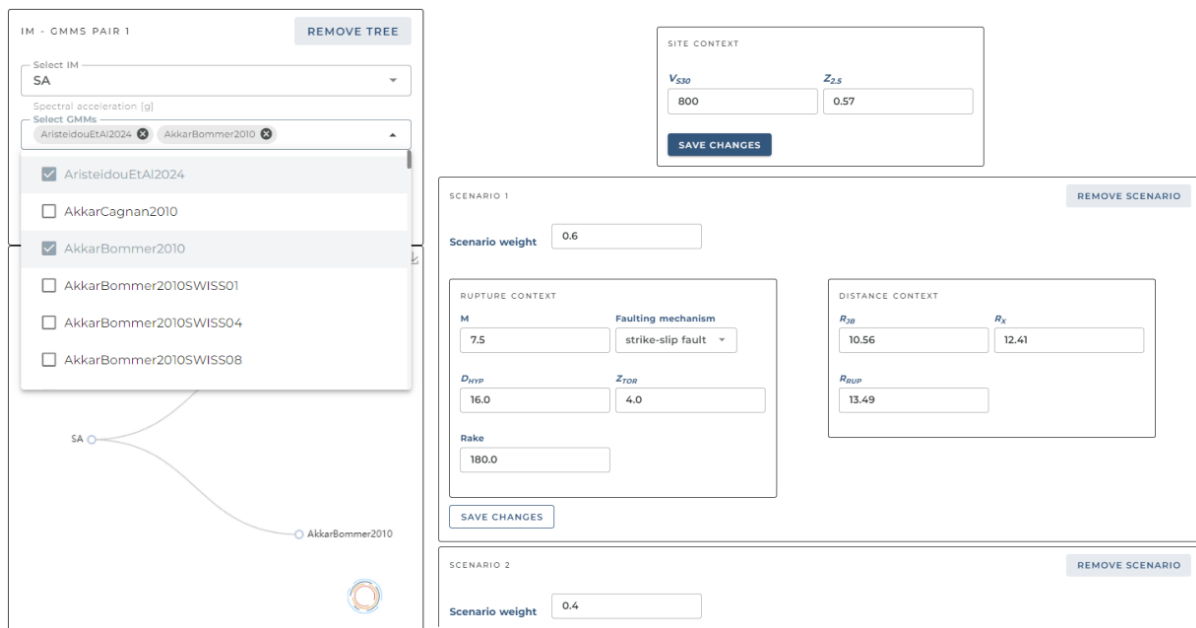


Figure 4. Graphical UI of the proposed tool: (left) IM-GMM pair selection, (right) Rupture scenario definition.

4. **Logic Tree:** after configuring the scenarios and finalising the input, the logic tree can be visualised. This takes the user to a dedicated page where all details about the IMs, GMMs, weights, rupture scenarios, and more are presented in a comprehensive table (Figure 5). This feature ensures that every aspect of the analysis is clearly organised and easily accessible. For a more intuitive overview, an interactive logic tree diagram (Figure 6) provides a global visual representation of the analysis. The diagram breaks down the different elements, beginning with the rupture scenarios (two in the provided example). For each rupture scenario, it illustrates the

IMs being predicted and the associated GMMs used to estimate their distributions. By hovering over individual elements, users can view specific weights assigned to the IMs and GMMs. The logic tree offers flexibility, allowing users to expand or collapse sections to display the desired level of detail. Additionally, both the full logic tree and the interactive diagram can be downloaded for offline use, providing a convenient way to store and review inputs and results.

5. **Advanced Input:** the software supports configuring several advanced input parameters, with default values pre-set for convenience. These configurations include selecting the number of horizontal components and the method used to define them (geomean, RotD100, RotD50) used to define them. Users can adjust the number of ground motions, set limits on scaling, and define computational settings, such as the number of iterations required to achieve a good match between the target distribution and the selected ground motions. Additionally, users can introduce more IM definitions, such as specifying $Sa(T)$ at a particular period, T , with the option to assign importance weights to each IM. Furthermore, causal earthquake rupture parameter limits can be customised to refine ground motion selections, for instance, by restricting to a particular magnitude range or faulting styles.

Logic Tree			
Q Search			
IM	GMM	Total weight	Causal parameters
SA	AristeidouEtAl2024	0.25	["d_hyp": 16, "gmms": [0, 1, 2], "mag": 7.5, "mechanism": "strike-slip fault", "rake": 180, "rjb": 1056, "rup": 1349, "rup_id": 0, "rx": 1241, "soil": 0, "vs30": 800, "z2pt5": 0.57, "ztor": 4]
SA	BooreAtkinson2008	0.25	["d_hyp": 16, "gmms": [0, 1, 2], "mag": 7.5, "mechanism": "strike-slip fault", "rake": 180, "rjb": 1056, "rup": 1349, "rup_id": 0, "rx": 1241, "soil": 0, "vs30": 800, "z2pt5": 0.57, "ztor": 4]
SA	AristeidouEtAl2024	0.25	["d_hyp": 16, "gmms": [0, 1, 2], "mag": 7.8, "mechanism": "strike-slip fault", "rake": 180, "rjb": 1056, "rup": 1349, "rup_id": 1, "rx": 1241, "soil": 0, "vs30": 800, "z2pt5": 0.57, "ztor": 4]
SA	BooreAtkinson2008	0.25	["d_hyp": 16, "gmms": [0, 1, 2], "mag": 7.8, "mechanism": "strike-slip fault", "rake": 180, "rjb": 1056, "rup": 1349, "rup_id": 1, "rx": 1241, "soil": 0, "vs30": 800, "z2pt5": 0.57, "ztor": 4]
Ds575	AristeidouEtAl2024	0.25	["d_hyp": 16, "gmms": [0, 1, 2], "mag": 7.5, "mechanism": "strike-slip fault", "rake": 180, "rjb": 1056, "rup": 1349, "rup_id": 0, "rx": 1241, "soil": 0, "vs30": 800, "z2pt5": 0.57, "ztor": 4]
Ds575	AbrahamsonSilva1996	0.25	["d_hyp": 16, "gmms": [0, 1, 2], "mag": 7.5, "mechanism": "strike-slip fault", "rake": 180, "rjb": 1056, "rup": 1349, "rup_id": 0, "rx": 1241, "soil": 0, "vs30": 800, "z2pt5": 0.57, "ztor": 4]
Ds575	AristeidouEtAl2024	0.25	["d_hyp": 16, "gmms": [0, 1, 2], "mag": 7.8, "mechanism": "strike-slip fault", "rake": 180, "rjb": 1056, "rup": 1349, "rup_id": 1, "rx": 1241, "soil": 0, "vs30": 800, "z2pt5": 0.57, "ztor": 4]
Ds575	AbrahamsonSilva1996	0.25	["d_hyp": 16, "gmms": [0, 1, 2], "mag": 7.8, "mechanism": "strike-slip fault", "rake": 180, "rjb": 1056, "rup": 1349, "rup_id": 1, "rx": 1241, "soil": 0, "vs30": 800, "z2pt5": 0.57, "ztor": 4]
PGV	AristeidouEtAl2024	0.1	["d_hyp": 16, "gmms": [0, 1, 2], "mag": 7.5, "mechanism": "strike-slip fault", "rake": 180, "rjb": 1056, "rup": 1349, "rup_id": 0, "rx": 1241, "soil": 0, "vs30": 800, "z2pt5": 0.57, "ztor": 4]
PGV	AkkarBommer2010	0.2	["d_hyp": 16, "gmms": [0, 1, 2], "mag": 7.5, "mechanism": "strike-slip fault", "rake": 180, "rjb": 1056, "rup": 1349, "rup_id": 0, "rx": 1241, "soil": 0, "vs30": 800, "z2pt5": 0.57, "ztor": 4]

Items per page: 10 1-10 of 14 < > >>

Figure 5. Logic tree table listing relevant data in a structured format.

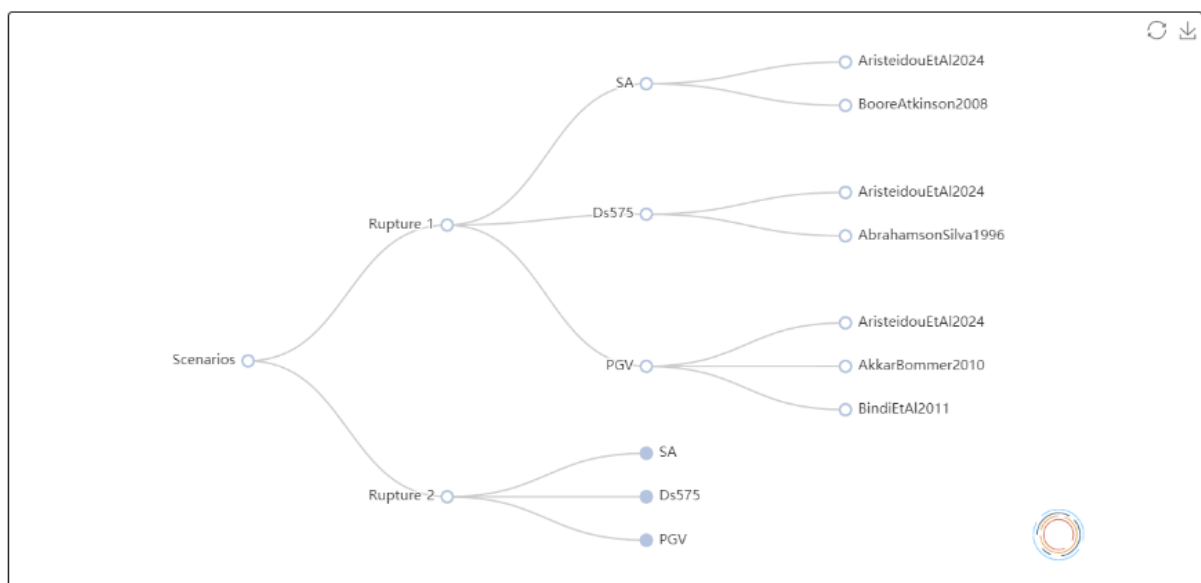


Figure 6. Interactive logic tree diagram.

It is important to note that at every step of input and output generation, data can be downloaded for use in other applications or analyses. Additionally, within the tool, additional hazard consistency checks may be performed.

5. Example unconditional and conditional record selection

Within this section, an example application of the tool and the framework described in Section 2 are presented. The tool is applied to perform selection following both methods: unconditional and conditional. Once, all input data is defined, the tool is used to generate a target distribution. Figure 7(left) demonstrates an example target unconditional distribution, while Figure 7(right) illustrates an example target conditional distribution, where IM^* corresponds to $Sa(0.7s)$ with a value of 0.3g. For the sample calculation, the scaling factors of the records were limited to 3.0, and magnitudes of the events were constrained to be 5 or higher.

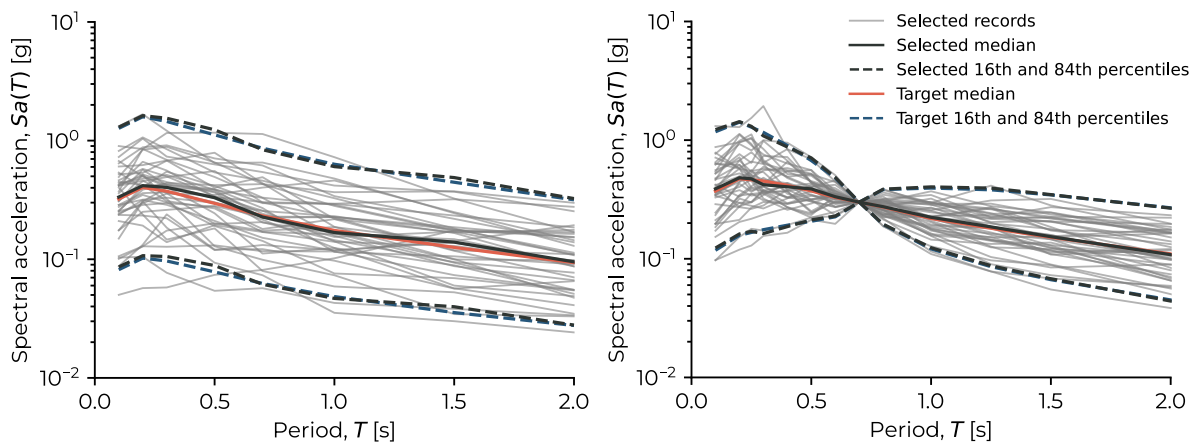


Figure 7. (left) unconditional and (right) conditional target distributions.

In addition to the target distributions, Figure 7 presents the selected record spectra and their median spectra. Each selected ground motion record spectrum is shown alongside the mean and standard deviations, which, as can be observed, correspond to the median and standard deviation of the target distributions. For each IM of interest, Kolmogorov-Smirnov (KS) goodness-of-fit tests are conducted to assess the quality of the selection. The KS test measures the absolute difference between the theoretical and cumulative distribution function (CDF) and the empirical distribution function (EDF) of the sample [22]. Figure 8 illustrates some of the IM tests, showing that the EDFs of the selected ground motions are representative of the target distribution and its KS bounds at a 5% significance level. Finally, the record suite can be downloaded for further analysis.

While it may be obvious, it is important to recall that there is no other software tool widely available that can perform such a ground motion record selection. That is, the ground motion characteristics in terms of the spectral acceleration, velocity, duration and more can all be targeted to be consistent with the seismic hazard of a given site. This essentially means that the chosen records are the more representative ground motions for that site of hazard based on the PSHA results. The benefit is that these ground motions are expected to be much more efficient (i.e., reduced dispersion in the structural response) and also eliminates any possible biasing of the results based on ground motion characteristics that are typically overlooked by practitioners, primarily because the appropriate tools were until now unavailable.

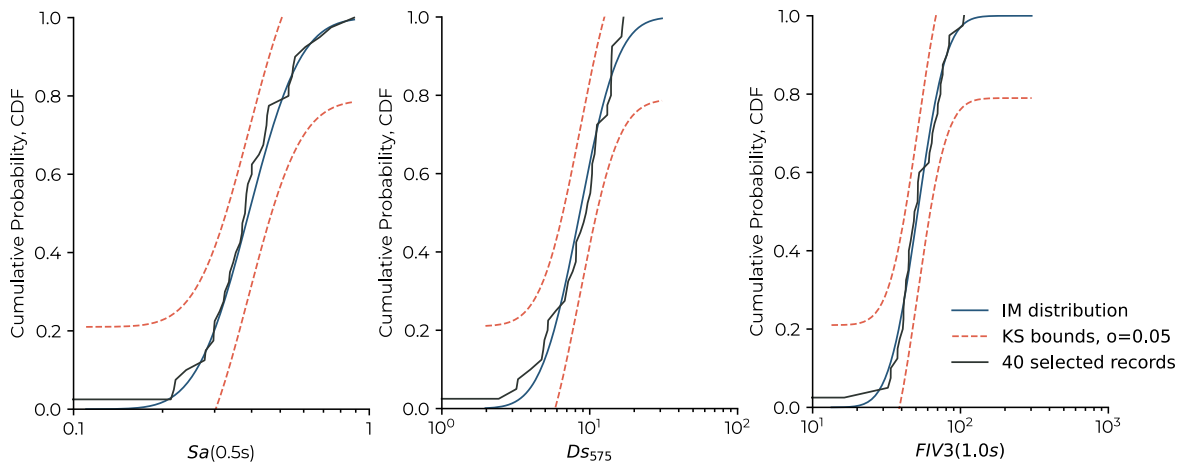


Figure 8. Illustration of the KS tests for a select IMs.

6. Summary

This paper introduced a user-friendly software tool designed to streamline the process of ground motion record selection for seismic design and assessment. By leveraging recent advancements in computational power, the software integrates state-of-the-art methods such as the ground motion conditional intensity measure (GCIM) framework, which allows for efficient record selection from harmonised databases like the PEER NGA-West2. It accommodates the use of multiple ground motion models (GMMs) and intensity measures (IMs) through cross-correlation matrices, mirroring the approach used in probabilistic seismic hazard analysis (PSHA). The tool offers flexibility in selecting both horizontal and vertical ground motion components and features a user interface (UI) that allows seamless switching between various methods of selection and easy retention of input and output data. A case study demonstrated the tool’s capabilities for both conditional and unconditional selection of ground motions. The approach was consistent with industry standards and provided a ground motions suite that matches the target distribution and passes all Kolmogorov-Smirnov goodness-of-fit tests for all IMs of interest that are reflected real-world conditions, making it particularly useful for site-specific studies and advanced ground motion selection methods incorporated in design codes.

Acknowledgements

The work presented in this paper has been developed within the framework of the project “Dipartimenti di Eccellenza 2023-2027”, funded by the Italian Ministry of Education, University and Research at IUSS Pavia.

Copyrights

3CroCEE 2025 reserves the copyright of the published proceedings. Authors will have the right to use the content of published papers, in part or in full, for their own work. Authors who use previously published data and illustrations must acknowledge the original source in the accompanying captions.

References

- [1] C. A. CORNELL, “Engineering Seismic Risk Analysis, *Bull. Seismol. Soc. Am.* 58, 1583–1606.,” *Bull. Seismol. Soc. Am.*, vol. 58, no. 5, pp. 1583–1606, 1968, [Online]. Available: <http://bssa.geoscienceworld.org/cgi/content/abstract/58/5/1583%5Cnhttp://bssaonline.org/cgi/content/abstract/58/5/1583>
- [2] J. W. Baker, “Conditional mean spectrum: Tool for ground-motion selection,” *J. Struct. Eng.*, vol. 137, no. 3, pp. 322–331, 2011, doi: 10.1061/(ASCE)ST.1943-541X.0000215.

- [3] T. Lin, S. C. Harmsen, J. W. Baker, and N. Luco, “Conditional Spectrum Computation Incorporating Multiple Causal Earthquakes and Ground-Motion Prediction Models,” *Bull. Seismol. Soc. Am.*, vol. 103, no. 2A, pp. 1103–1116, Apr. 2013, doi: 10.1785/0120110293.
- [4] N. Jayaram, T. Lin, and J. W. Baker, “A Computationally Efficient Ground-Motion Selection Algorithm for Matching a Target Response Spectrum Mean and Variance,” *Earthq. Spectra*, vol. 27, no. 3, pp. 797–815, Aug. 2011, doi: 10.1193/1.3608002.
- [5] G. Wang, “A ground motion selection and modification method capturing response spectrum characteristics and variability of scenario earthquakes,” *Soil Dyn. Earthq. Eng.*, vol. 31, no. 4, pp. 611–625, Apr. 2011, doi: 10.1016/j.soildyn.2010.11.007.
- [6] B. A. Bradley, “A generalized conditional intensity measure approach and holistic ground-motion selection,” *Earthq. Eng. Struct. Dyn.*, vol. 39, no. 12, pp. 1321–1342, Oct. 2010, doi: 10.1002/eqe.995.
- [7] B. A. Bradley, “A ground motion selection algorithm based on the generalized conditional intensity measure approach,” *Soil Dyn. Earthq. Eng.*, vol. 40, pp. 48–61, Sep. 2012, doi: 10.1016/j.soildyn.2012.04.007.
- [8] B. A. Bradley, “Empirical equations for the prediction of displacement spectrum intensity and its correlation with other intensity measures,” *Soil Dyn. Earthq. Eng.*, vol. 31, no. 8, pp. 1182–1191, Aug. 2011, doi: 10.1016/j.soildyn.2011.04.007.
- [9] K. Afshari and J. P. Stewart, “Physically Parameterized Prediction Equations for Significant Duration in Active Crustal Regions,” *Earthq. Spectra*, vol. 32, no. 4, pp. 2057–2081, Nov. 2016, doi: 10.1193/063015EQS106M.
- [10] K. W. Campbell and Y. Bozorgnia, “Ground Motion Models for the Horizontal Components of Arias Intensity (AI) and Cumulative Absolute Velocity (CAV) Using the NGA-West2 Database,” *Earthq. Spectra*, vol. 35, no. 3, pp. 1289–1310, Aug. 2019, doi: 10.1193/090818EQS212M.
- [11] H. Zafarani and M. R. Soghrat, “Ground Motion Models for Non-Spectral Intensity Measures Based on the Iranian Database,” *J. Earthq. Eng.*, vol. 27, no. 13, pp. 3786–3806, Oct. 2023, doi: 10.1080/13632469.2022.2150334.
- [12] H. Dávalos, P. Heresi, and E. Miranda, “A ground motion prediction equation for filtered incremental velocity, FIV3,” *Soil Dyn. Earthq. Eng.*, vol. 139, p. 106346, Dec. 2020, doi: 10.1016/j.soildyn.2020.106346.
- [13] H. Dávalos and E. Miranda, “A Ground Motion Prediction Model for Average Spectral Acceleration,” *J. Earthq. Eng.*, vol. 25, no. 2, pp. 319–342, Jan. 2021, doi: 10.1080/13632469.2018.1518278.
- [14] H. Dávalos and E. Miranda, “Filtered incremental velocity: A novel approach in intensity measures for seismic collapse estimation,” *Earthq. Eng. Struct. Dyn.*, vol. 48, no. 12, pp. 1384–1405, Oct. 2019, doi: 10.1002/eqe.3205.
- [15] L. Eads, E. Miranda, and D. G. Lignos, “Average spectral acceleration as an intensity measure for collapse risk assessment,” *Earthq. Eng. Struct. Dyn.*, vol. 44, no. 12, pp. 2057–2073, Sep. 2015, doi: 10.1002/eqe.2575.
- [16] G. J. O’Reilly, “Seismic intensity measures for risk assessment of bridges,” *Bull. Earthq. Eng.*, vol. 19, no. 9, pp. 3671–3699, Jul. 2021, doi: 10.1007/s10518-021-01114-z.
- [17] S. Aristeidou, D. Shahnazaryan, and G. J. O’Reilly, “Artificial neural network-based ground motion model for next-generation seismic intensity measures,” *Soil Dyn. Earthq. Eng.*, vol. 184, p. 108851, Sep. 2024, doi: 10.1016/j.soildyn.2024.108851.
- [18] S. Aristeidou, D. Shahnazaryan, and G. J. O’Reilly, “Correlation models for next-generation

- amplitude and cumulative intensity measures using artificial neural networks,” *Earthq. Spectra*, Oct. 2024, doi: 10.1177/87552930241270563.
- [19] T. D. Ancheta *et al.*, “NGA-West2 database,” *Earthq. Spectra*, vol. 30, no. 3, pp. 989–1005, 2014, doi: 10.1193/070913EQS197M.
- [20] J. W. Baker and B. A. Bradley, “Intensity Measure Correlations Observed in the NGA-West2 Database, and Dependence of Correlations on Rupture and Site Parameters,” *Earthq. Spectra*, vol. 33, no. 1, pp. 145–156, Feb. 2017, doi: 10.1193/060716eqs095m.
- [21] N. Jayaram and J. W. Baker, “Efficient sampling and data reduction techniques for probabilistic seismic lifeline risk assessment,” *Earthq. Eng. Struct. Dyn.*, vol. 39, no. 10, pp. 1109–1131, Aug. 2010, doi: 10.1002/eqe.988.
- [22] A. H.-S. Ang and W. H. Tang, *Probability Concepts in Engineering: Emphasis on Applications in Civil and Environmental Engineering*. New York, NY: Wiley, 2006.